Inorg. Chem. **1982**, *21*, 2630-2636

Contribution from the Departments of Chemistry, The Johns Hopkins University, Baltimore, Maryland 21218,
and Emory University, Atlanta, Georgia 30322

Coordinating Properties of Alkylated 6-Aminopurines. Electrostatic Potential Distributions for 3-Methyladenine and 9-Methyladenine and Preparation and Structure of *cis*-Diamminebis(3-methyladenine)platinum(II) Nitrate Trihydrate

JOHN D. ORBELL,[1a] CARMEN SOLORZANO,[1a] LUIGI G. MARZILLI,*[1b] and THOMAS J. KISTENMACHER*[1a]

Received October 6, 1981

Electrostatic potential maps have been computed for 3-methyladenine and 9-methyladenine under the INDO molecular orbital approximation. These maps clearly indicate a shift in the attractive electrophilic site from N(1) of the six-membered pyrimidine ring to N(7) of the five-membered imidazole ring and a marked increase in molecular dipole moment on going from the 9-substituted to the 3-substituted purine. These features help to rationalize the increased ligating power of 3-alkylated 6-aminopurines over 9-alkylated 6-aminopurines. The synthesis, solution ^{1}H NMR spectrum, and solid-state molecular and crystal structure of *cis*-diamminebis(3-methyladenine)platinum(II) nitrate trihydrate, *cis*-$[(NH_3)_2Pt(3\text{-MeA})_2](NO_3)_2\cdot 3H_2O$, are also reported. The compound crystallizes in the triclinic system, space group $P\bar{1}$, with a = 10.877 (4) Å, b = 15.395 (5) Å, c = 7.604 (2) Å, α = 103.33 (2)°, β = 102.90 (2)°, γ = 99.94 (2)°, V = 1173.6 Å^3, Z = 2 (based on a molecular weight of 705.52 for $[Pt(NH_3)_2(C_6N_5H_7)_2](NO_3)_2\cdot 3H_2O$), D_{measd} = 1.99 (1) g cm^{-3}, and D_{calcd} = 1.99 g cm^{-3}. The crystal structure was solved by conventional Patterson and Fourier methods and refined by full-matrix least-squares techniques to an R value of 0.044. The *cis*-$[(NH_3)_2Pt(3\text{-MeA})_2]^{2+}$ cation is essentially square planar with the two independent 3-MeA ligands showing N(7)–Pt bonding and is arranged in a head-to-tail fashion such that the complex cation possesses approximate C_2 molecular symmetry. Principal geometrical parameters are as follows: Pt–N(ammine) = 2.039 (6) Å, 2.031 (6) Å; Pt–N(7)(3-MeA) = 2.010 (4) Å, 2.004 (4) Å; N(ammine)–Pt–N(ammine) = 90.6 (2)°; N(7)–Pt–N(7) = 89.5 (2)°; interbase dihedral angle = 90.6°; base/PtN$_4$ coordination plane dihedral angle = 98.9, 111.8°. The extended crystal structure exhibits two different types of base-stacking interactions and two different kinds of base pairing through hydrogen bonds. There is also an extensive network of hydrogen bonds. Further stabilization is afforded by base/nitrate anion stacking. The ^{1}H NMR spectrum of the platinated 3-MeA ligand is compared to that of the free base and to the spectra of several Co(III)–3-alkylated 6-aminopurine complexes. The present complex affords a model for an N(7)$_{5'\text{-AMP}}$–Pt–N(7)$_{5'\text{-AMP}}$ type cross-linking mode that is perhaps applicable to the binding of Pt(II) antitumor drugs to DNA. It is suggested that such a cross-link would demand about the same degree of local denaturation of a polynucleotide as one of the type N(7)$_{5'\text{-GMP}}$–Pt–N(7)$_{5'\text{-GMP}}$.

Introduction

Alkylation may occur at any number of endo- or exocyclic heteroatoms of purine bases. The relative degree and position of alkylation can greatly affect such physiochemical properties as dipole moment (and hence base-stacking strength and pattern),[2] hydrogen-bonding capability,[2] and metal-coordinating propensity.[3,4] For example, we examined the relative formation constants (K_f) for the binding of alkylated adenines to the bis(acetylacetonato)nitrocobalt(III) moiety.[3,4] A singular aspect of these studies was the rather marked increase ($\Delta(\log K_f) \approx 2$) for 3-substituted 6-aminopurines (3-RA) over 9-substituted 6-aminopurines (9-RA). Later, we found[5] that 3-alkylated 6-aminopurines have ligating power sufficient to react readily with the sterically restrictive cobaloxime system $LCo(DH)_2X$ (where L = an easily substituted neutral ligand as Me$_2$SO, DH = the monoanion of dimethylglyoxime, and X = an anionic ligand exhibiting a strong trans influence such as an alkyl or a phosphonate [(O)P(OR)$_2$]) to yield stable, isolable complexes of the type $[(3\text{-RA})Co(DH)_2X]$.

In the present study, this work is extended to the investigation of the binding of 3-methyladenine (3-MeA), Figure 1, to the *cis*-$[(NH_3)_2Pt^{II}]^{2+}$ species. Model systems involving cis coordination of two nucleobases to the A_2Pt^{II} cationic moiety, where A = NH$_3$ or A$_2$ = ethylenediamine (en) or trimethylenediamine (tn), have been extensively investigated in attempts to gain insights into the binding of Pt(II) antitumor drugs to DNA.[6,7] Particular attention has been given to the possibility of an inter- or intrastrand cross-link as the critical lesion.[6,7] The stability order of (diethylenetriamine-palladium(II) binding to the purine nucleoside 5′-monophosphates quantitatively shows[8] a distinct preference for the N(7) site of 5′-GMP (guanosine 5′-monophosphate) over either the N(1) or N(7) sites of 5′-AMP (adenosine 5′-monophosphate). These results are surely applicable to Pt(II),[8] in spite of earlier data[9] that suggested approximately equivalent binding of $[(NH_3)_2Pt(H_2O)_2]^{2+}$ to 5′-GMP and 5′-AMP. However, cross-links of the type N(7)$_{5'\text{-AMP}}$–Pt–N(7)$_{5'\text{-AMP}}$, N(1)$_{5'\text{-AMP}}$–Pt–N(1)$_{5'\text{-AMP}}$, or N(1)$_{5'\text{-AMP}}$–Pt–N(7)$_{5'\text{-AMP}}$ are not devoid of interest, since kinetically the formation of a critical lesion may occur at sites other than those thermodynamically favored. Perhaps, then, in part because of the poorer coordinating properties of 5′-AMP and because of the availability of two base binding sites (N(1) and N(7)) that can lead to mixtures of isomers and posssibly to oligomers, no *cis*-bis(6-aminopurine)platinum(II) complex has yet been subjected to detailed examination by X-ray crystallography. In contrast, such studies on *cis*-bis(6-oxopurine)platinum(II) complexes abound.[6,7]

In light of the above considerations, it occurred to us that once again we could exploit the enhanced N(7) donor ability of 3-substituted 6-aminopurines to prepare and examine a

---

(1) (a) The Johns Hopkins University. (b) Emory University.

(2) (a) Shugar, D.; Szer, W. *J. Mol. Biol.* **1962**, *5*, 580. (b) Ts'O, P. O. P.; Chan, S. I. *J. Am. Chem. Soc.* **1964**, *86*, 4176. (c) Helmkamp, G. K.; Kondo, N. S. *Biochim. Biophys. Acta* **1968**, *157*, 242. (d) Brennan, T.; Weeks, C.; Shefter, E.; Rao, S. T.; Sundaralingam, M. *J. Am. Chem. Soc.* **1972**, *94*, 8548 and references therein.

(3) Sorrell, T.; Epps, L. A.; Kistenmacher, T. J.; Marzilli, L. G. *J. Am. Chem. Soc.* **1977**, *99*, 2173.

(4) Sorrell, T.; Epps, L. A.; Kistenmacher, T. J.; Marzilli, L. G. *J. Am. Chem. Soc.* **1978**, *100*, 5756.

(5) Toscano, P. J.; Chiang, C. C.; Kistenmacher, T. J.; Marzilli, L. G. *Inorg. Chem.* **1981**, *20*, 1513.

(6) de Castro, B.; Kistenmacher, T. J.; Marzilli, L. G. In "Trace Elements in the Pathogenesis and Treatment of Inflammatory Conditions"; Rainsford, K. D., Brune, K., Whitehouse, M. W., Eds.; Agents and Actions: Basel, 1981; and references therein.

(7) (a) Marzilli, L. G.; Kistenmacher, T. J.; Eichhorn, G. L. In "Nucleic Acid-Metal Ion Interactions"; Spiro, T. G., Ed.; Wiley: New York, 1980; Chapter 5. (b) Barton, J. K.; Lippard, S. J. *Ibid.*, Chapter 2. (c) Marzilli, L. G. *Adv. Inorg. Biochem.* **1981**, *3*.

(8) Vestues, P. I.; Martin, R. B. *J. Am. Chem. Soc.* **1981**, *103*, 806.

(9) Scovell, W. M.; O'Connor, T. J. *J. Am. Chem. Soc.* **1977**, *99*, 120; *Chem.-Biol. Interact.* **1979**, *26*, 227.

0020-1669/82/1321-2630$01.25/0

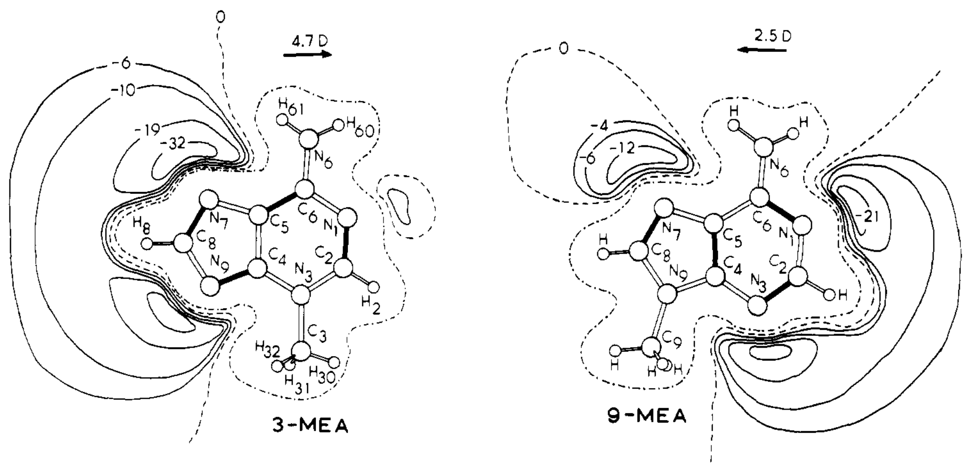

Figure 1. Molecular structures of the modified 6-aminopurine bases 3-methyladenine and 9-methyladenine. In each case, contour lines (in kcal mol^{-1}) are given for the in-plane electrostatic potential as computed by the INDO method. Relative magnitudes and directions (also obtained by the INDO method) of the molecular dipole moments are indicated.

model for an $N(7)_{5'\text{-AMP}}$–Pt–$N(7)_{5'\text{-AMP}}$ cross-link. This has been successful, and we have characterized the title complex *cis*-$[(NH_3)_2Pt(3\text{-MeA})_2](NO_3)_2 \cdot 3H_2O$ by X-ray diffraction and ^1H NMR spectroscopy. Also described are some of the differences in the electronic structures of 3- and 9-substituted 6-aminopurine ligands, which allow a semiquantitative understanding of the variance in the coordinating abilities of these two types of alkylated purine bases.

Experimental Section

(a) Reagents. The 3-MeA free base was synthesized according to a literature procedure.[3,4,10,11] Common chemicals were obtained from scientific supply houses.

(b) Preparation of *cis*-$[(NH_3)_2Pt(3\text{-MeA})_2](NO_3)_2 \cdot 3H_2O$. An aqueous 3-mL solution of 0.28 g of $AgNO_3$ (1.6 mmol) was added to a suspension of 0.40 g (0.8 mmol) of *cis*-$(NH_3)_2PtI_2$[12] in 5–10 mL of distilled water. The resulting suspension was gently heated with stirring at 60 °C for 30 min, and the insoluble AgI was removed by filtration through Celite. The pale yellow filtrate was heated to 65 °C, and a warm dilute aqueous/dimethylformamide solution (6 mL, 65 °C) containing 0.25 g of 3-methyladenine (3-MeA) (1.6 mmol) was added with stirring. The pH of the final solution was ca. 5. The solution was stirred for 1 h at 80 °C. After several days of slow evaporation at room temperature, 0.15 g of white precipitate was collected by filtration. The precipitate was then recrystallized from hot water as colorless platelets. A density measurement ($CCl_4/CHBr_3$) and preliminary X-ray data were consistent with the formulation $[(NH_3)_2Pt(3\text{-MeA})_2](NO_3)_2 \cdot 3H_2O$. This was later confirmed by the full X-ray analysis.

It is noted, however, that a bulk chemical analysis is more consistent with a formulation of the compound as the dihydrate. Anal. Calcd for $PtN_{14}C_{12}O_8H_{24}$: N, 28.52; C, 20.96; H, 3.52. Found: N, 28.52; C, 20.99; H, 3.53.

(c) ^1H NMR Data. ^1H NMR data, obtained from crystals of the title compound dissolved in $Me_2SO\text{-}d_6$ and referenced to Me_4Si, were collected on a Varian T60 spectrometer.

(d) Collection and Reduction of the X-ray Intensity Data. Oscillation and Weissenberg photography showed the crystal class to be triclinic and allowed the computation of preliminary unit-cell data. A single, well-formed crystal was selected for intensity data collection and cleaved parallel to the (001) plane to give a platelet with the following faces and mean dimensions: (001)–($00\bar{1}$), 0.22 mm; (110)–($\bar{1}\bar{1}0$), 0.24 mm; ($1\bar{1}0$)–($\bar{1}10$), 0.07 mm. Precise unit-cell dimensions, together with their standard deviations, were derived from a least-squares fit to the setting angles for 15 carefully selected reflections centered on a Syntex $P\bar{1}$ automated diffractometer. The crystallographic *c* axis was approximately aligned along the ϕ axis of the spectrometer.

Table I. Crystal Data for *cis*-$[(NH_3)_2Pt(3\text{-MeA})_2](NO_3)_2 \cdot 3H_2O$

$a = 10.877$ (4) Å	$V = 1173.6$ Å^3
$b = 15.395$ (5) Å	formula $[Pt(NH_3)_2(C_6N_5H_7)_2](NO_3)_2 \cdot 3H_2O$
$c = 7.604$ (2) Å	space group $P\bar{1}$
$\alpha = 103.33$ (2)°	mol wt = 705.52
$\beta = 102.90$ (2)°	$D_{\text{measd}} = 1.99$ (1) g cm^{-3}
$\gamma = 99.94$ (2)°	D_{calcd} ($Z = 2$) = 1.99 g cm^{-3}

Pertinent crystallographic data are collected in Table I. With the employment of graphite-monochromatized Mo Kα radiation (λ = 0.71069 Å) and the use of the θ–2θ scan mode with a variable scan rate of 2.0–8.0° min^{-1}, the intensities of 7276 reflections (including standards) in the $+h$ hemisphere were surveyed to $2\theta = 60°$. Three standards were monitored after every 50 reflections and showed no systematic variation over the course of the experiment. Out of a unique set of 6894 reflections, 6661 had net intensities above zero, and these were assigned observational variances on the basis of the equation $\sigma^2(I) = S + (B_1 + B_2)(T_S/2T_B)^2 + (pI)^2$, where S, B_1, and B_2 are the scan and extremum background counts, T_S and T_B are the scan and individual background counting times ($T_B = T_S/2$), and p, which represents an estimate of the error proportional to the diffracted intensity,[13] was given a value of 0.03.

The nonzero intensities and their estimated standard deviations were corrected for Lorentz and polarization effects and for the effect of absorption (Gaussian integration, 8 × 8 × 8 grid). On the basis of the above face assignments and crystal dimensions and a calculated linear absorption coefficient of 63.5 cm^{-1}, the maximum and minimum transmission factors were 0.66 and 0.26, respectively. An approximation to the absolute scale factor was derived by the method of Wilson.[14]

(e) Solution and Refinement of the Structure. The positional coordinates of the Pt atom were deduced from a three-dimensional Patterson synthesis, space group $P\bar{1}$ assumed. A subsequent structure factor/Fourier calculation allowed the location of the 36 other nonhydrogen atoms. Several cycles of isotropic and anisotropic least-squares refinement, minimizing the quantity $\sum w(|F_o| - |F_c|)^2$ where $w = 4F_o^2/\sigma^2(F_o^2)$, gave an R value ($=\sum||F_o| - |F_c||/\sum|F_o|$) of 0.052. At this stage, a difference-Fourier synthesis yielded coordinates for all H atoms except those associated with the three waters of crystallization. The isotropic thermal parameters of the located H atoms were fixed at a value ca. 1.0 Å^2 larger than that for the atom to which it was bonded. Two subsequent cycles of refinement, holding the H atom parameters fixed, led to convergence (maxiumum shift/error of 0.6) and to a final R value of 0.044. The final weighted R value ($=(\sum w(|F_o| - |F_c|)^2/\sum w|F_o|^2)^{1/2}$) and goodness of fit ($=(\sum w(|F_o| - |F_c|)^2/(NO - NV))^{1/2}$, where NO = 6661 nonzero observations and NV = 310 variables) were 0.050 and 1.8, respectively. A final difference-Fourier map was essentially featureless, with the exception of a peak at a height of 3.4 e Å^{-3} near the Pt atom site.

---

(10) Zorbach, W. W., Tipson, R. S., Eds. "Synthetic Procedures in Nucleic Acid Chemistry"; Interscience: New York, 1968; Vol. 1.

(11) Fox, J. R. Ph.D. Dissertation, University of Illinois, 1965.

(12) Dhara, S. C. *Indian J. Chem.* **1970**, *8*, 193.

(13) Busing, W. R.; Levy, H. A. *J. Chem. Phys.* **1957**, *26*, 563.

(14) Wilson, A. J. C. *Nature (London)* **1942**, *150*, 152.

Table II. Final Nonhydrogen Atom Coordinates for *cis*-$[(NH_3)_2Pt(3\text{-}MeA)_2](NO_3)_2\cdot 3H_2O$[a]

atom	*x*	*y*	*z*	atom	*x*	*y*	*z*
Pt[b]	62993 (2)	82068 (1)	86884 (2)	N(9B)	9322 (5)	6803 (3)	9066 (6)
N(10)	7294 (5)	9235 (3)	7909 (8)	C(2B)	11399 (6)	8563 (4)	13129 (8)
N(11)	4668 (6)	8685 (4)	8142 (7)	C(3B)	11963 (7)	7160 (6)	11572 (11)
N(1A)	3332 (6)	5168 (3)	5184 (6)	C(4B)	9874 (5)	7558 (3)	10548 (7)
N(3A)	3146 (5)	4975 (3)	8106 (6)	C(5B)	9025 (5)	8131 (3)	10761 (7)
N(6A)	4637 (5)	6449 (3)	4901 (6)	C(6B)	9413 (5)	8920 (3)	12325 (7)
N(7A)	5278 (4)	7138 (3)	9258 (5)	C(8B)	8143 (5)	6947 (3)	8378 (7)
N(9A)	4430 (4)	6228 (3)	10861 (5)	N(41)	8830 (7)	7793 (4)	5283 (8)
C(2A)	2858 (6)	4715 (4)	6252 (8)	O(41)	9432 (7)	8514 (4)	6613 (8)
C(3A)	2536 (7)	4428 (4)	9177 (9)	O(42)	9511 (7)	7261 (4)	4689 (9)
C(4A)	3979 (5)	5809 (3)	9002 (6)	O(43)	7609 (6)	7609 (4)	4636 (8)
C(5A)	4484 (5)	6342 (3)	7962 (6)	N(51)	5067 (6)	9179 (4)	3254 (8)
C(6A)	4171 (5)	6006 (3)	6003 (6)	O(51)	4149 (6)	9186 (4)	1948 (7)
C(8A)	5204 (5)	7019 (3)	10932 (6)	O(52)	6142 (8)	9632 (5)	3426 (14)
N(1B)	10639 (4)	9124 (3)	13444 (6)	O(53)	4860 (7)	8701 (4)	4322 (8)
N(3B)	11083 (5)	7774 (3)	11761 (7)	O(W1)	546 (10)	5590 (6)	6930 (14)
N(6B)	8633 (5)	9457 (3)	12775 (7)	O(W2)	1998 (11)	7270 (7)	6529 (15)
N(7B)	7898 (4)	7734 (3)	9324 (6)	O(W3)	1814 (11)	8981 (7)	8932 (15)

[a] Estimated standard deviations in the least significant figure are enclosed in parentheses in this and in all the following tables. [b] Parameters are $\times 10^5$; for all other atoms, parameters are $\times 10^4$.

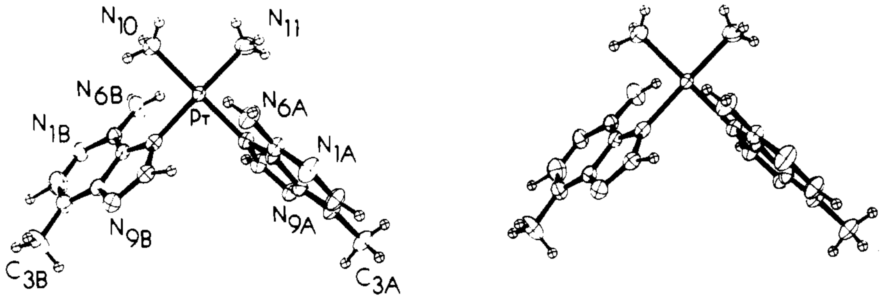

Figure 2. Stereoview approximately normal to the mean coordination plane for the *cis*-$[(NH_3)_2Pt(3\text{-}MeA)_2]^{2+}$ cation.

Neutral-atom scattering curves for the nonhydrogen atoms[15] and the H atoms[16] were taken from common sources. Anomalous dispersion corrections were applied to the scattering curves for all nonhydrogen atoms.[17] Final atomic coordinates for the nonhydrogen atoms are collected in Table II. Tables of anisotropic thermal parameters, parameters for the H atoms, and final observed and calculated structure-factor amplitudes are available.[18] The crystallographic computations were performed with a standard set of computer programs.[19]

Results and Discussion

Qualitative Electronic Structures for 3-Methyladenine and 9-Methyladenine. The electronic properties of the substituted purines 3-methyladenine and 9-methyladenine (9-MeA) have been explored with the INDO molecular orbital approximation.[20,21] From these computations, we derive the molecular dipole moment and the molecular electrostatic potential (Figure 1). The main results of these computations can be summarized as follows.

(A) 9-Methyladenine. The computed molecular dipole moment at 2.5 D is in excellent agreement with other semiempirical estimates[22a] and in good accord with experiment[23] (3.0 D, with CCl_4 as the solvent). The order of preference for electrophilic attack (as denoted by its electrostatic potential[24]) is N(1) ≈ N(3) > N(7) as suggested by earlier results for adenine.[22a] Metal-binding studies also suggest a preference for attack at N(1) or N(7), with the N(3) site mitigated against by the presence of the bulky methyl substituent at N(9).[7]

(B) 3-Methyladenine. The shift in the methyl substitution site from N(9) to N(3) of the 6-aminopurine framework causes dramatic change in both the molecular dipole moment and the molecular electrostatic potential (Figure 1). The computations yield a theoretical moment for 3-methyladenine that is nearly a factor of 2 larger[22b] (4.7 vs. 2.5 D) and oriented approximately opposite in direction to that computed for 9-methyladenine. We know of no experimental determination of the dipole moment of 3-methyladenine. Similarly, the order of preference for electrophilic attack is substantially altered, with N(7) being clearly favored over N(1).[22b] The N(9) site, which is essentially electronically equivalent to N(7), is now mitigated against by the presence of the methyl substituent at N(3).

(C) Consequences. The well depth in the electrostatic potential at N(7) of 3-MeA is computed to be at least 11 kcal

---

(15) Hanson, H. P.; Herman, F.; Lea, J. D.; Skillman, S. *Acta Crystallogr.* **1964**, *17*, 1040.

(16) Stewart, R. F.; Davidson, E. R.; Simpson, W. T. *J. Chem. Phys.* **1965**, *42*, 3175.

(17) Cromer, D. T.; Liberman, D. *J. Chem. Phys.* **1970**, *53*, 1891.

(18) See paragraph at end of the paper regarding supplementary material.

(19) Crystallographic programs employed include Wehe, Busing, and Levy's ORABS, Zalkin's FORDAP, Busing, Martin, and Levy's ORFLS (modified), Pippy and Ahmed's MEAN PLANE, and Johnson's ORTEP.

(20) (a) Pople, J. A.; Segal, G. A. *J. Chem. Phys.* **1966**, *44*, 3289. (b) The limitations of approximate molecular orbital methods for the calculation of electrostatic potentials have been explored (Geissner-Prettre, C.; Pullman, A. *Theor. Chim. Acta* **1972**, *25*, 83; **1974**, *33*, 91; **1975**, *36*, 335). On the basis of the considerations contained in these papers, the comparison of the electrostatic potentials of 3-MeA and 9-MeA with each other is probably considerably more reliable than either potential individually.

(21) (a) The molecular geometry employed for the 9-MeA molecule was that found in its crystal structure (Kistenmacher, T. J.; Rossi, M. *Acta Crystallogr., Sect. B* **1977**, *B33*, 253). (b) Similarly, the geometry of the 3-MeA molecule was assimilated from that of 3-ethyladenine in its solid-state structure (Petersen, C. H.; Furberg, S. *Acta Chem. Scand., Ser. B* **1975**, *B29*, 37).

(22) (a) Berthod, H.; Geissner-Prettre, C.; Pullman, A. *Theor. Chim. Acta* **1966**, *5*, 53. (b) Denis, A.; Berthod, H. *J. Chim. Phys. Phys.-Chim. Biol.* **1968**, *65*, 1815.

(23) De Voe, H.; Tinoco, I. *J. Mol. Biol.* **1962**, *4*, 500.

(24) Bonaccorsi, R.; Pullman, A.; Scrocco, E.; Tomasi, J. *Theor. Chim. Acta* **1972**, *24*, 51.

Table III. Molecular Geometry for *cis*-$[(NH_3)_2Pt(3\text{-}MeA)_2](NO_3)_2\cdot 3H_2O$

(a) Primary Coordination Sphere about the Pt Atom

Bond Lengths (Å)			
Pt–N(10)	2.039 (6)	Pt–N(7A)	2.010 (4)
Pt–N(11)	2.031 (6)	Pt–N(7B)	2.004 (4)
Bond Angles (Deg)			
N(10)–Pt–N(11)	90.6 (2)	N(1)–Pt–N(7A)	89.3 (2)
N(10)–Pt–N(7A)	175.8 (2)	N(11)–Pt–N(7B)	177.8 (2)
N(10)–Pt–N(7B)	90.8 (2)	N(7A)–Pt–N(7B)	89.5 (2)

(b) 3-Methyladenine Bases

	A	B
Bond Lengths (Å)		
N(1)–C(2)	1.317 (8)	1.315 (8)
N(1)–C(6)	1.362 (7)	1.351 (7)
N(3)–C(2)	1.321 (8)	1.336 (8)
N(3)–C(3)	1.476 (8)	1.464 (10)
N(3)–C(4)	1.361 (7)	1.363 (7)
N(6)–C(6)	1.327 (7)	1.328 (7)
N(7)–C(5)	1.384 (6)	1.380 (7)
N(7)–C(8)	1.345 (7)	1.361 (7)
N(9)–C(4)	1.347 (7)	1.355 (7)
N(9)–C(8)	1.338 (7)	1.348 (7)
C(4)–C(5)	1.394 (7)	1.392 (7)
C(5)–C(6)	1.400 (7)	1.414 (7)
Bond Angles (Deg)		
Pt–N(7)–C(8)	129.2 (4)	127.5 (4)
Pt–N(7)–C(5)	126.5 (3)	129.1 (3)
C(5)–N(7)–C(8)	104.3 (4)	103.4 (4)
C(2)–N(1)–C(6)	119.2 (5)	119.8 (5)
C(2)–N(3)–C(3)	122.4 (5)	122.7 (6)
C(4)–N(3)–C(3)	120.6 (5)	121.0 (5)
C(2)–N(3)–C(4)	116.9 (5)	116.3 (5)
C(4)–N(9)–C(8)	102.9 (4)	102.4 (4)
N(1)–C(2)–N(3)	126.5 (6)	126.1 (6)
N(3)–C(4)–C(5)	119.9 (5)	121.0 (5)
N(3)–C(4)–N(9)	128.7 (5)	127.7 (5)
N(9)–C(4)–C(5)	111.5 (4)	111.3 (5)
C(6)–C(5)–N(7)	134.1 (5)	134.0 (5)
C(5)–C(6)–N(6)	124.3 (5)	123.7 (5)
N(1)–C(6)–N(6)	118.2 (5)	118.4 (5)
C(5)–C(6)–N(1)	117.5 (5)	118.0 (5)
N(7)–C(8)–N(9)	115.4 (5)	115.7 (5)

mol^{-1} more favorable than those for N(1) or N(7) of 9-MeA. The main result of the differences in the electrostatic potentials for 3-MeA and 9-MeA may well lie, however, in the selection of the site of electrophilic attack. While metal attack at N(1) or N(7) of 9-substituted 6-aminopurines is about equally probable, N(7) can be considered the "preferred" site of metal attack for 3-MeA.

These arguments allow then a simplistic rationalization of the differences in the coordinating properties of 3-MeA and 9-MeA for which there is experimental evidence.[3,4] Moreover, they help to clarify and quantify ideas we have presented earlier[3,4,25] and exploited here and elsewhere[5] for the rational synthesis and study of elusive metal complexes of 6-aminopurines.

Molecular Geometry of the *cis*-$[(NH_3)_2Pt(3\text{-}MeA)_2]^{2+}$ Cation. This first successful synthesis and crystallization of a *cis*-bis(6-aminopurine)platinum(II) complex allows an important opportunity to study in detail a model for a $N(7)_{5'\text{-}AMP}$–Pt–$N(7)_{5'\text{-}AMP}$ cross-link. Of particular interest is a comparison (vide infra) between the conformational properties of this model complex and those exhibited by models for the $N(7)_{5'\text{-}GMP}$–Pt–$N(7)_{5'\text{-}GMP}$ lesion.[6,7]

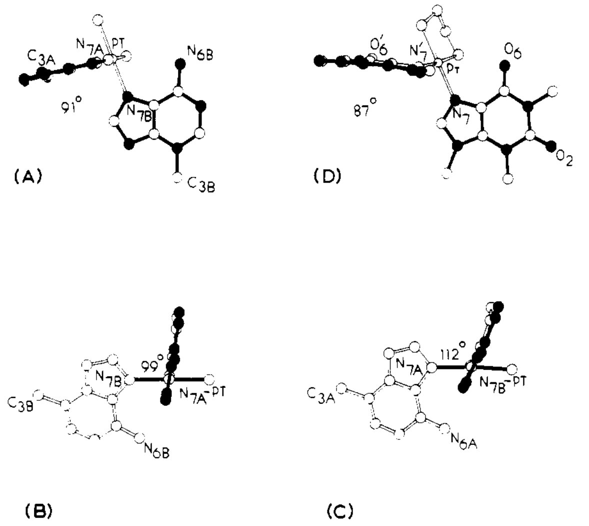

Figure 3. Illustrations of the principal molecular conformational properties of the *cis*-$[(NH_3)_2Pt(3\text{-}MeA)_2]^{2+}$ cation: (A) the base/base dihedral angle; (B and C) the base/PtN_4 coordination plane dihedral angles. Also included is an illustration (D) of the interplanar dihedral angle in the $[(en)Pt(1,3,9\text{-}TMX)_2]^{2+}$ cation for obvious comparison with (A).

The molecular geometry of the *cis*-$[(NH_3)_2Pt(3\text{-}MeA)_2]^{2+}$ cation in the present salt is depicted in the stereoview of Figure 2. The coordination geometry about the Pt(II) center is nominally square planar, with the four equatorial sites being occupied by the N(7) atoms of two cis-bound 3-MeA ligands (labeled A and B) and the N atoms of two ammine ligands ($N(10)H_3$ and $N(11)H_3$). The two 3-MeA ligands are arranged in a head-to-tail fashion such that the cation possesses approximate C_2 molecular symmetry (see below).

Bond lengths and bond angles for the complex cation are collected in Table III. The Pt–N(7A) and Pt–N(7B) bond lengths at 2.010 (4) and 2.004 (4) Å are in excellent internal agreement and appear to be shorter by ca. 0.02–0.04 Å than has been typically found for Pt–N(7) bond lengths in 6-oxopurine complexes with an ammine ligand trans to the purine base.[6,7,26] This difference, if significant, could easily be related to the strong coordinating ability of the 3-MeA base as noted above. A more meaningful comparison to Pt–N(7) bond lengths for 9-substituted 6-aminopurine complexes is presently unavailable, as only values for two other complexes have been reported ($[Cl_3(9\text{-}MeA)Pt^{II}]^-$, Pt–N(7) = 2.015 (4) Å,[27] and $[(\mu\text{-}9\text{-}MeA)((i\text{-}Pr)_2SO)_2Pt^{II}]^{2+}$, Pt–N(7) = 2.07 (3) Å and Pt–N(1) = 2.08 (3) Å[28]). Neither of the Pt–N(7) distances in these two complexes is directly comparable to the present case, owing to overall charge considerations and the nature of the ligand trans to the substituted adenine ligand. The remaining bond lengths and angles in the primary coordination sphere are typical of those found in other Pt(II) complexes.[6,7,26]

As indicated above, one of our principal interests in the present complex cation is as a model for the $N(7)_{5'\text{-}AMP}$–Pt–$N(7)_{5'\text{-}AMP}$ cross-link. We have described a convention[29] for the most important geometrical parameters, namely, the interbase dihedral angle (B/B′), the base/PtN_4 coordination plane dihedral angles (B/PtN_4 and B′/PtN_4), and the perpendicular displacement of the Pt atom from the base to which it is bonded (Δ_{Pt} from base B and Δ_{Pt}' from base B′). For the

---

(25) Kistenmacher, T. J. In "Chemical Applications of Atomic and Molecular Electrostatic Potentials"; Politzer, P., Truhlar, D. G., Eds.; Plenum Press: New York, 1981; pp 445–467.

(26) Orbell, J. D.; Wilkowski, K.; de Castro, B.; Marzilli, L. G.; Kistenmacher, T. J. *Inorg. Chem.* **1982**, *21*, 813.

(27) (a) Terzis, A.; Hadjiliadis, N.; Rivest, R.; Theophanides, T. *Inorg. Chim. Acta* **1975**, *12*, L5. (b) Terzis, A. *Inorg. Chem.* **1976**, *15*, 793.

(28) Lock, C. J. L.; Speranzini, R. A.; Turner, G.; Powell, J. *J. Am. Chem. Soc.* **1976**, *98*, 7865.

(29) Orbell, J. D.; Marzilli, L. G.; Kistenmacher, T. J. *J. Am. Chem. Soc.* **1981**, *103*, 5126.

Table IV. Least-Squares Planes and the Deviation of Individual Atoms (Å) from These Planes for *cis*-$[(NH_3)_2Pt(3\text{-}MeA)_2](NO_3)_2 \cdot 3H_2O^a$

(a) Primary Coordination Sphere
$(0.0787X - 0.3062Y - 0.9487Z = -8.8531$ Å)

Pt	−0.017	N(10)	0.056
N(7A)	0.058	N(11)	−0.048
N(7B)	−0.048		

(b) Imidazole Ring A
$(0.8850X - 0.4633Y + 0.0474Z = -1.7960$ Å)

N(9A)	0.001	C(5A)	0.004
N(7A)	−0.004	C(8A)	0.002
C(4A)	−0.003		

(c) Imidazole Ring B
$(-0.4378X - 0.6797Y + 0.5885Z = -4.9141$ Å)

N(9B)	0.005	C(5B)	0.008
N(7B)	−0.004	C(8B)	−0.001
C(4B)	−0.008		

(d) Pyrimidine Ring A
$(0.8778X - 0.4740Y + 0.0686Z = -1.7551$ Å)

N(1A)	0.007	C(3A)	−0.055*
N(3A)	0.008	C(4A)	0.008
N(6A)	0.034*	C(5A)	−0.016
C(2A)	−0.016	C(6A)	0.009

(e) Pyrimidine Ring B
$(-0.4131X - 0.7011Y + 0.5812Z = -5.0080$ Å)

N(1B)	−0.010	C(3B)	0.089*
N(3B)	0.018	C(4B)	0.004
N(6B)	0.153*	C(5B)	−0.027
C(2B)	−0.015	C(6B)	0.031

(f) 3-Methyladenine Ligand A
$(0.8803X - 0.4704Y + 0.0615Z = -1.7612$ Å)

N(1A)	0.015	C(3A)	−0.078*
N(3A)	−0.003	C(4A)	−0.003
N(6A)	0.053*	C(5A)	−0.016
N(7A)	−0.020	C(6A)	0.018
N(9A)	0.017	C(8A)	0.009
C(2A)	−0.018	Pt	−0.050*

(g) 3-Methyladenine Ligand B
$(-0.4230X - 0.6946Y + 0.5819Z = -5.0049$ Å)

N(1B)	−0.003	C(3B)	0.056*
N(3B)	0.002	C(4B)	−0.003
N(6B)	0.185*	C(5B)	−0.017
N(7B)	−0.031	C(6B)	0.047
N(9B)	0.028	C(8B)	0.002
C(2B)	−0.024	Pt	−0.141*

[a] In each of the equations of the planes, X, Y, and Z are coordinates referred to the orthogonal axes: X along the a axis, Y in the ab plane, and Z along the c^* axis. Atoms designated by an asterisk were given zero weight in calculating the planes; the atoms used to define the planes were given equal weight.

cis-$[(NH_3)_2Pt(3\text{-}MeA)_2]^{2+}$ cations, these conformational parameters are as follows: B/B′ dihedral angle of 90.6°, the B,B′/PtN_4 dihedral angles of 98.9° for ligand A and 111.8° for ligand B, and Pt atom displacements of −0.05 Å for ligand A and −0.14 Å for ligand B (Table IV). Illustrations of the conformational dihedral angles for the 3-MeA complex cation are presented in Figure 3A–C.

The large B/B′ dihedral angle of 90.6° (Figure 3A) is suggestive of little intramolecular base/base interaction, in spite of a favorably large molecular dipole moment in free 3-MeA. Presumably, the molecular conformation adopted in the crystal is determined by a competition between intracomplex and intercomplex interactions, with the intercomplex interactions probably predominating. It has been suggested that intramolecular steric factors in *cis*-bis(6-oxopurine)platinum(II) complexes are considerably less determinative of the resultant molecular conformation than those in *cis*-bis(pyrimidine) complexes of Pt(II).[26,29,30] Steric factors are determined by the number and type of exocyclic functional groups on the C atoms α to the metal-binding site.[26,29,30] For N(7)-bound purine complexes, the only functional groups adjacent to the metal-binding site are H atoms, whether the base is a 6-oxo- or a 6-aminopurine. Thus, there is a range of energetically available values for the B/B′ dihedral angles (and likewise for the B/PtN_4 angles) for *cis*-bis(purine)platinum(II) complexes. It is interesting to note, however, that the molecular conformational parameters in the present complex are similar to those displayed[26] by the PF_6^- salt of *cis*-[(ethylenediamine)bis(1,3,9-trimethylxanthine)platinum(II)](2+)—a complex cation that shows C_2 molecular symmetry in the solid, a B/B′ dihedral angle of 87.3°, a value of 121.4° for the one independent B/PtN_4 dihedral angle, and a displacement of the Pt atom from the purine plane by −0.22 Å; the B/B′ dihedral angle for the 1,3,9-trimethylxanthine complex is illustrated in Figure 3D. Close similarity between the molecular conformations of the 3-MeA complex and the PF_6^- salt of the 1,3,9-trimethylxanthine complex should not be too heavily weighted as it was noted previously[26] that a substantial conformational change takes place on crystallizing the xanthine-containing cation as its NO_3^- salt.

We anticipate, then, that there is considerable conformational freedom in *cis*-bis(6-aminopurine) as well as *cis*-bis(6-oxopurine) complexes of Pt(II). Thus, the structural perturbation of a DNA molecule upon binding of the *cis*-$(NH_3)_2Pt^{II}$ moiety in a cross-linking mode involving N(7) of two 5′-AMP units need not be dissimilar to that induced by a mode involving N(7) of two 5′-GMP units. Both of these cross-links would, of course, demand some degree of local denaturation or premelting in order to accommodate their formation. In either case, however, the steric demands are unlikely to be as restrictive as those envisioned for an $N(3)_{5'\text{-CMP}}$–Pt–$N(3)_{5'\text{-CMP}}$ cross-link, where intramolecular steric effects predominate and fix the B/B′ dihedral angle at a large value (>100°).[29]

Molecular Dimensions of the 3-Methyladenine Ligands and the Nitrate Anions. Bond lengths and angles for the two independent 3-MeA ligands are compared in Table III. There are no significant differences in the bond lengths for the two ligands A and B and only two significantly different bond angles, namely, Pt–N(7)–C(8) and Pt–N(7)–C(5). The variance in these exocyclic bond angles is probably a direct result of the different environments about each ligand. The molecular dimensions given here for the 3-methyladenine bases compare favorably with those reported for the 3-substituted 6-aminopurines triacanthine (3-(γ,γ-dimethylallyl)-6-aminopurine)[31] and 3-ethyladenine[21b] and the Co(III) complexes of 3-benzyladenine[5] and triacanthine.[4] There is, however, a slight distortion of the imidazole ring in the coordinated bases as reflected in a widening of the C(5)–N(7)–C(8), C(4)–N(9)–C(8), and C(6)–C(5)–N(7) bond angles and a decrease in the N(7)–C(8)–N(9) angle relative to the same angles in the free bases.

The nine-atom frameworks of the two 3-MeA ligands in the present complex are measurably nonplanar (Table IV). The dihedral angles between the five-membered imidazole and the six-membered pyrimidine ring are 1.2 (3) and 2.0 (3)° for ligands A and B, respectively. Displacements of the exocyclic functional groups (including the coordinated Pt atom) are also given in Table IV.

The two symmetry-independent NO_3^- anions show, as commonly found, evidence for librational disorder, with the

---

(30) Kistenmacher, T. J.; de Castro, B.; Wilkowski, K.; Marzilli, L. G. *J. Inorg. Biochem.* **1982**, *16*, 33.

(31) Kistenmacher, T. J.; Urmey, W. F.; Rossi, M. *J. Cryst. Mol. Struct.* **1977**, *7*, 219.

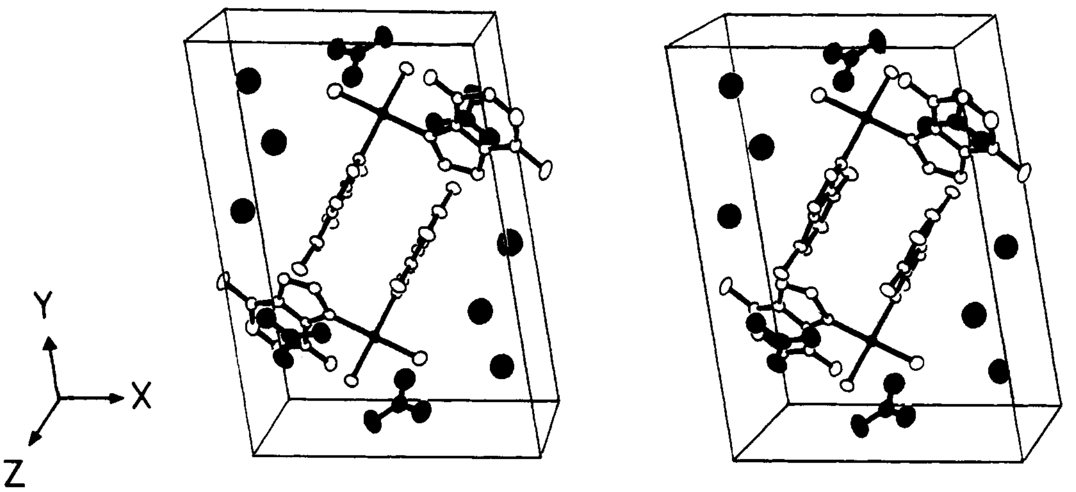

Figure 4. Stereoview of the crystal packing in *cis*-$[(NH_3)_2Pt(3\text{-}MeA)_2](NO_3)_2 \cdot 3H_2O$. Hydrogen atoms on the complex cation have been omitted for clarity; hydrogen atoms on the waters of crystallization were not located.

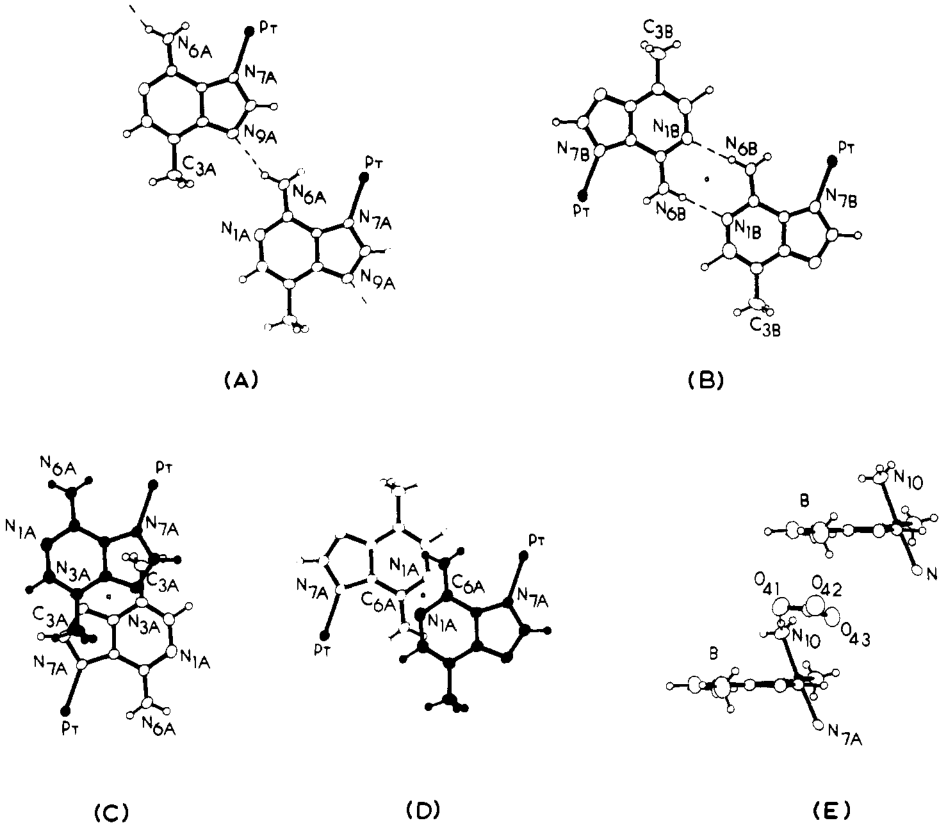

Figure 5. Principal intermolecular interactions in the crystal structure of *cis*-$[(NH_3)_2Pt(3\text{-}MeA)_2](NO_3)_2 \cdot 3H_2O$: (A) the ribbons of hydrogen bonds along *c* involving the 3-MeA ligand labeled A; (B) the centrosymmetric hydrogen-bond dimers involving the 3-MeA ligand labeled B; (C and D) base-stacking interactions for ligand A; (E) base(ligand B)/nitrate/base(ligand B) columns propagating along *c*.

oxygen atoms of these anions exhibiting varying degrees of exaggerated thermal motion. We have made no attempt to "correct" the observed dimensions for thermal effects. The average uncorrected N–O bond length is 1.25 (2) Å (range 1.22–1.27 Å), and the average uncorrectd O–N–O bond angle is 120 (2)° (range 116.7–122.2°).

Extended Crystal Structure. An illustration of the unit-cell contents for *cis*-$[(NH_3)_2Pt(3\text{-}MeA)_2](NO_3)_2 \cdot 3H_2O$ is presented in the stereoview of Figure 4. The extended crystal structure is characterized by a network of hydrogen bonds involving the water molecules of crystallization, the oxygen atoms of the nitrate anions, the exocyclic amino group, the endocyclic N(1) and N(9) atoms of the purine ligands, and the coordinated ammines $N(10)H_3$ and $N(11)H_3$. Possible hydrogen-bonding interactions are collected in Table V.

Two types of interbase hydrogen bonding are observed in the structure and illustrated in Figure 5A,B. For ligand A, a ribbon of interbase hydrogen bonds propagates along the crystallographic *c* axis, utilizing the exocyclic amino group as the donor and the ring site N(9) as the acceptor. Coupling of ligands of type B into hydrogen-bonded dimers about centers of symmetry are also observed; in this dimeric coupling, the exocyclic amino group again acts as the donor and now the ring site N(1) acts as the acceptor. In addition to its interbase hydrogen bonding, ligand A also shows two types of interbase stacking about centers of inversion (Figure 5C,D). In each case, the base/base overlap is slight and the interplanar distances (3.47 Å in Figure 5C and 3.52 Å in Figure 5D) are

Table V. Distances (Å) and Angles (Deg) in Interactions of the Type D–H···A

D	H	D–H	A[a]	H···A	D···A	D–H···A
N(10)	H(102)	0.935	O(41)[b]	2.069	3.003 (8)	177
N(10)	H(100)	0.831	O(W3)[c]	2.225	3.042 (8)	168
N(10)	H(101)	0.840	O(51)[d]	2.624	3.107 (8)	118
N(10)	H(101)	0.840	O(53)[b]	2.521	3.180 (8)	136
N(11)	H(111)	0.862	O(51)[e]	2.289	3.023 (8)	143
N(11)	H(112)	0.856	O(53)[b]	2.466	2.964 (8)	130
N(11)	H(112)	0.856	O(W2)[b]	2.570	3.111 (8)	122
N(6A)	H(60A)	0.878	N(9A)[f]	2.161	2.964 (8)	152
N(6B)	H(61B)	0.871	N(1B)[g]	2.173	3.026 (8)	166
N(6B)	H(60B)	0.876	O(52)[e]	2.363	2.907 (8)	121
O(W1)			N(9B)		2.885 (8)	
O(W1)			O(W1)		2.927 (8)	
O(W2)			O(W1)		2.906 (8)	
O(W2)			O(42)		2.750 (8)	
O(W3)			O(W2)		2.906 (8)	
O(W3)			O(41)		2.660 (8)	
O(W3)			O(51)		2.932 (8)	

[a] All superscripts in this column refer to symmetry transforms (space group $P\overline{1}$). [b] x, y, z. [c] $1-x, 2-y, 2-z$. [d] $1-x, 2-y, 1-z$. [e] $x, y, 1+z$. [f] $x, y, z-1$. [g] $2-x, 2-y, 3-z$.

typical of a van der Waals separation.

Additional crystal stability is, of course, afforded by the electrostatic interactions between the complex cations and the NO_3^- anions. In particular, we note the interaction between one of the nitrate anions, $N(41)O_3$, and ligand B (Figure 5E), allowing the sandwiching of the nitrate anion by two B ligands. We also note that this interaction is augmented by a weak hydrogen bond between the ammine ligand $N(10)H_3$ and O(41) of the sandwiched nitrate anion (N(10)···O(41) = 3.003 (8) Å). The dihedral angle between the plane of the nitrate anion and that of ligand B is 14°.

^{1}H NMR Results. Relevant ^{1}H NMR chemical shift data for crystals of *cis*-$[(NH_3)_2Pt(3\text{-}MeA)_2](NO_3)_2\cdot 3H_2O$ dissolved in $Me_2SO\text{-}d_6$ are compared to shift data for other complexed and free 3-alkylated 6-aminopurines in Table VI. The amino resonance in the title complex is a broad singlet as in uncomplexed 3-MeA[4] and the other uncoordinated 3-alkylated 6-aminopurine bases,[4] indicating free rotation about the N(6)–C(6) bond on the NMR time scale. This is consistent with the absence of intramolecular hydrogen bonding involving the exocyclic amino group. Such intramolecular hydrogen bonding is responsible for the two distinct signals observed for the exocyclic amino protons in the acac complexes[4] listed in Table VI. We note, however, that the NH_2 resonance is shifted downfield considerably, even though this group is not coordinated to the Pt. In addition, there is a relatively large shift downfield for the H(8) resonance (consistent with preferential N(7) binding) and a moderately large downfield shift for the H(2) resonance (Table VI). Similar H(2) shifts are also observed for the acac complexes,[4] but there the H(8) shifts are small. The shift pattern for the title complex is the same, however, as those found for the oxime compounds,[5] although the shift magnitudes are much less in the latter.

Table VI. Comparison of ^{1}H NMR Chemical Shifts for Free and Complexed 3-Alkylated 6-Aminopurine Bases[a]

	–H(2)	–H(8)	$-NH_2$
(1) Free Bases			
triacanthine (Tria)[b]	8.30	7.75	7.82
3-benzyladenine (3-BzA)[b]	8.53	7.75	7.90
3-methyladenine (3-MeA)[b]	8.25	7.73	~7.76
(2) Coordinated Bases			
$[(Tria)Co(acac)_2(NO_2)]$[b]	8.55	7.79	7.97, 8.63
$[(3\text{-}BzA)Co(acac)_2(NO_2)]$[b]	8.82	7.82	8.04, 8.72
$[(3\text{-}BzA)Co(DH)_2X]$ (X = CH_3 or $P(O)(OCH_3)_2$)[c]	~8.60	~7.89	*d*
$[(3\text{-}MeA)Co(acac)_3(NO_2)]$[b]	8.47	7.77	7.94, 8.51
$[(NH_3)_2Pt(3\text{-}MeA)_2](NO_3)_2$[e]	8.42	8.12	8.75

[a] Chemical shifts in ppm from Me_4Si with $Me_2SO\text{-}d_6$ as the solvent. [b] Taken from ref 4. [c] Taken from ref 5. [d] Too broad to be observed. [e] This work. The ammine resonance is observed as a broad singlet at 4.42 ppm. The 3-methyl resonance is observed as a sharp singlet at 3.76 ppm.

Clearly in these inert metal complexes, the shift patterns are complicated by heavy-atom effects of the metal. Interpretation of metal-binding sites based on NMR shift data obviously requires care.

Summary. The preparation and some of the physical properties of the coordination compound *cis*-$[(NH_3)_2Pt(3\text{-}MeA)_2](NO_3)_2\cdot 3H_2O$ are reported. The conformation of the complex cation (exemplified by its B/B′ and B,B′/PtN$_4$ dihedral angles) is qualitatively similar to some *cis*-bis(6-oxopurine)platinum(II) complexes. In both cases the observed molecular conformation is likely to arise from a competition between intramolecular and intermolecular interactions, with intermolecular interactions probably predominating. Thus, deformations of a DNA duplex by cross-links of the type $N(7)_{5'\text{-AMP}}\text{–Pt–}N(7)_{5'\text{-AMP}}$ and $N(7)_{5'\text{-GMP}}\text{–Pt–}N(7)_{5'\text{-GMP}}$ need not be different.

Acknowledgment. This investigation was supported by the National Institutes of Health, Public Health Service Grant GM 29222. We thank Matthey Bishop, Inc., for a loan of K_2PtCl_4.

Registry No. *cis*-$[(NH_3)_2Pt(3\text{-}MeA)_2](NO_3)_2\cdot 3H_2O$, 81391-15-3; *cis*-$(NH_3)_2PtI_2$, 15978-93-5; 3-methyladenine, 5142-23-4; 9-methyladenine, 700-00-5.

Supplementary Material Available: Tables of nonhydrogen atom anisotropic thermal parameters, parameters for the hydrogen atoms, calculated and observed structure factor amplitudes, and "atom-in-molecule" charges (INDO approximation) for 9-methyladenine and 3-methyladenine (45 pages). Ordering information is given on any current masthead page.